

Combined Engine for Reusable Launch Vehicle (KLIN Cycle)

V. V. Balepin*

MSE Technology Applications, Inc., Butte, Montana 59702

P. A. Czysz†

St. Louis University, St. Louis, Missouri 63103

and

R. H. Moszée‡

U.S. Air Force Research Laboratory, Edwards Air Force Base, California 93524

Predicted performance and features of a combined propulsion concept for a small reusable launch vehicle known as KLIN™ (meaning *wedge* in Russian) Cycle are discussed. The KLIN Cycle consists of a thermally integrated deeply cooled turbojet and a liquid rocket engine. The objective of this concept is to achieve a high-pressure ratio in a simple, lightweight turbojet engine. The proven result is an exceptional engine thrust-to-weight ratio, as well as improved specific impulse and mass fraction of the launcher. When based on the RL10 engine family, the KLIN Cycle makes a small single-stage-to-orbit and two-stage-to-orbit reusable launch vehicles feasible and very economically attractive.

Nomenclature

C_O^A	= oxygen mass concentration in atmospheric air
DOL	= deeply cooled turbojet (DCTJ) thrust fraction in total KLIN Cycle thrust
G_H	= hydrogen flow rate
I_{sp}	= specific impulse
I_{sp}^E	= effective specific impulse
I_{TJ}	= DCTJ specific impulse
K_A	= ratio of the airflow rate and total [liquid rocket engine (LRE) fuel and turbojet fuel]
K_O	= oxygen/hydrogen stoichiometric ratio
K_X	= oxygen/hydrogen mixture ratio in LRE
\dot{M}_A^{TJ}	= mass of the DCTJ per 1 kilogram per second of airflow
p_{st}	= steam partial pressure
R	= engine thrust
T/W	= thrust-to-weight ratio
T_T	= turbine temperature
X	= vehicle drag
ξ	= hydrogen distribution factor between the turbojet and LRE
ϕ	= fraction of the injected oxygen in the air/oxygen mixture
ψ	= LRE throttling factor

Introduction

THE aerospace community seeks innovative approaches to develop technologies that can double existing rocket propulsion capabilities by the year 2010 through specific impulse I_{sp} and mass fraction improvement and relatively low life-cycle costs. One attractive solution is a propulsion system that integrates an existing liquid rocket engine (LRE) with a deeply cooled turbojet (DCTJ), or the so-called KLIN™ (meaning *wedge* in Russian) Cycle. This approach makes feasible systems that are not feasible with all-rocket propulsion [small or middle-class reusable single-stage-to-orbit (SSTO) launchers]. A KLIN Cycle-based launcher can create a new mar-

ket of on-demand, small payload launch services, similar to Federal Express® or United Parcel Service®. Additionally, it can boost space commerce activities, including space manufacturing.

Liquid-air-cycle engine derivatives and DCTJ propulsion technology are listed among the four top priorities for detailed study in the National Research Council 1998 Report.¹

Concept Description

In the proposed KLIN cycle liquid hydrogen fuel for the rocket and the turbojet engines is used to deeply cool inlet air to 110 K at sea-level conditions and to 200–250 K at Mach 6. The flow diagram in Fig. 1 shows integration of the DCTJ with an LRE of the RL10 family. Because the air is deeply cooled, a high pressure ratio is attainable with simple (single spool) and lightweight turbomachinery. This results in high cycle performance and an extremely high thrust-to-weight ratio for an airbreathing propulsion system.

The KLIN Cycle incorporates several rocket and DCTJ units. All of the DCTJ units and all or part of the LRE units operate from takeoff. The LRE units may be throttled or even shutdown for a portion of the trajectory after initial acceleration, returning to full use when the DCTJ units are shutdown. The DCTJ units are intended for operation from takeoff with a gradual reduction in thrust output until they are finally shutdown at Mach 6–6.5. The DCTJ units will be newly designed turbomachines incorporating a lightweight compressor optimized for low-temperature operation.

For a small launcher the high-performance family of RL10 rocket engines is an appropriate choice. Low-cycle pressure and some features of configuration make the RL10 an ideal candidate for integration into the KLIN Cycle. The RL10 engine uses an expander cycle; therefore, it can be “naturally” integrated into the KLIN Cycle.

When using additional heat provided by the air precooler, a reduction in hydrogen peak pressure is a possibility. In turn, hydrogen pressure reduction is a favorable factor for KLIN Cycle reliability. If additional heat is used to increase chamber pressure, an RL10 thrust increase of up to 16% and a sea-level I_{sp} increase of up to 3% can be realized (Estimation for this study was done by United Technologies Research Center/Pratt and Whitney.). The higher thrust 50,000-lbf approximately 23 tons RL50 engine recently announced by the Pratt and Whitney Company could also be applied to a small reusable launch vehicle (RLV) propulsion system. According to *Aviation Week & Space Technology*, 21 June 1999, this “engine is to cost about what an RL10 does, \$5–\$10 million (depending on which version), but offers approximately twice the thrust.”

The KLIN Cycle offers very flexible performance characteristics and represents a unique compromise between engine weight and

Received 26 July 2000; revision received 22 November 2000; accepted for publication 29 December 2000; presented as Paper 01-1911 at the 10th International Space Planes and Hypersonic Systems and Technologies Conference, Kyoto, Japan, 24–27 April 2001. Copyright © 2001 by the American Institute of Aeronautics and Astronautics, Inc. All rights reserved.

*Staff Scientist, Aerospace Group.

†Professor, Department of Aerospace and Mechanical Engineering.

‡Senior Aerospace Engineer, Propulsion Directorate.

fuel efficiency that provides a high payload capability for the vertical takeoff launcher.

Figure 2 shows examples of the flight scenarios of the turbojet-dominated KLIN Cycle (Fig. 2a) with an air-to-hydrogen ratio $K_A = 12$ and a rocket-dominated KLIN Cycle (Fig. 2b) with $K_A = 4$, as profiles of relative thrust and relative KLIN Cycle-rocket I_{sp} . The data in Fig. 2a are presented on a logarithmic scale. Preferable operation modes and parameters are discussed next.

With the KLIN Cycle various launchers [e.g., SSTO, two-stage-to-orbit with fly-back booster], as well as different takeoff and landing scenarios (horizontal or vertical, including a powered descent and landing), are possible.

A small reusable vertical takeoff/horizontal landing SSTO launcher that delivers a 330-lb payload to a 220 n miles, 28.5-deg inclination orbit was selected as the baseline launcher concept in this study. The values presented correspond to requirements for NASA's BANTAM Lifter.

Advantages of the KLIN Cycle can be summarized as follows:

1) It is a simple configuration. Ideas such as an air/oxygen heat exchanger for additional air cooling, helium closed loop, or the bypass turbojet were rejected from the beginning of the concept analysis in order to maintain a simple design. Turbomachinery of the simplest possible configuration was considered, and a single spool design with no variable geometry for the compressor was employed. The addition of these features will definitely improve turbojet parameters, but they will also add mass and complexity.

2) It uses near-term technology. The reliable precooler is probably the most advanced component.

3) It has a lightweight structure caused by the high efficiency of air processing (high specific thrust), "excess" of cooling hydrogen, and a low-temperature compact compressor.

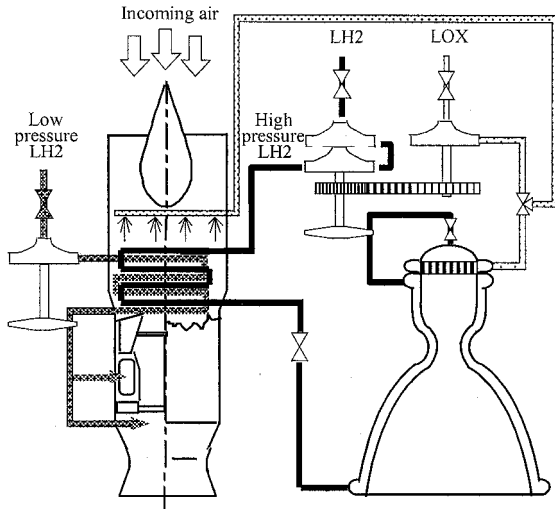


Fig. 1 Basic configuration of the RL10-based KLIN Cycle.

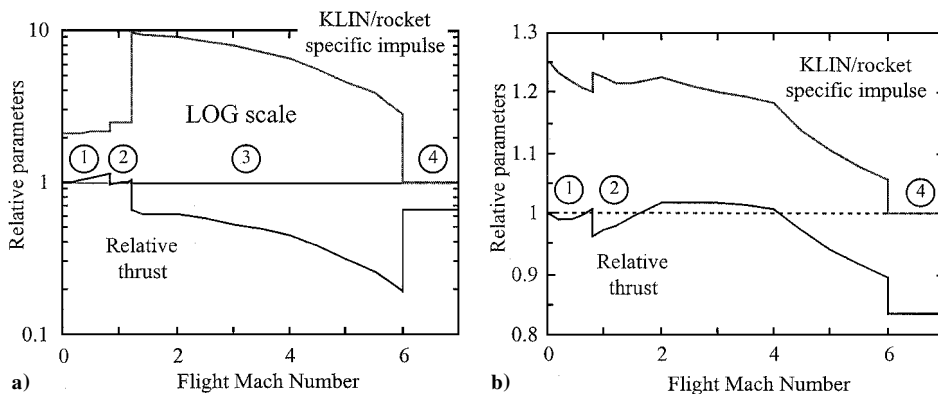


Fig. 2 Thrust and I_{sp} profile for a) turbojet-dominated and b) rocket-dominated KLIN Cycles: 1) LRE and liquid oxygen-augmented DCTJ operation; 2) LOX augmentation cutoff; 3) DCTJ sole operation; and 4) LRE sole operation.

4) It has a high engine thrust-to-weight ratio.

5) It has a two to three times higher I_{sp} than for an LRE depending on the mission [the Integrated High Payoff Rocket Propulsion Technology Program goal for year 2010 is a 26% I_{sp} improvement.

6) It has a known solution for the icing problem.

In Ref. 2 an oxygen-augmented DCTJ was considered. Subcooled liquid oxygen (LOX) was proposed to inject in front of the precooler. The main objective of oxygen injection at low flight altitude is to reduce air temperature in front of the precooler below the water triple point. As shown in Ref. 3, no precooler icing is expected at the air stagnation temperature in front of the precooler T_a^{in} below 273 K and at steam partial pressure p_{st} below the steam pressure in the triple point p_{tr} ($p_{tr} = 0.00623$ atm). These two conditions define seasonal speed-altitude limits of icing, and these analytical considerations were confirmed by experimental studies at the Central Institute of Aviation Motors in Russia, as well as in the sea level static (SLS) test of the precooled Japanese air turbo ramjet (ATREX) engine (Ref. 3). For the KLIN-Cycle simulation it was assumed that oxygen is injected into the airflow in front of the precooler from SLS to Mach ≈ 0.8 .

Another advantage of oxygen augmentation is a DCTJ thrust increase with almost no change in precooler and compressor hardware. Thus, oxygen injection in the amount of 10% of airflow leads to a thrust increase of approximately 20%.

Main Parameters

The main parameters of the scheme defining performance and mass of the propulsion system are $\xi = G_H^{TJ}/G_H^{\Sigma}$, and $\varphi = G_{OX}/(G_A + G_{OX})$. The air-to-hydrogen ratio, hydrogen distribution factor, and oxygen fraction define equivalence mixture ratio as

$$E = \frac{\xi K_0}{K_A [C_O^A + \varphi/(1 - \varphi)]} \quad (1)$$

where $K_0 = 7.937$, and $C_O^A = 0.2315$. For the standard air temperature 288 K, 4% of oxygen is enough to chill air to the water triple point if injected oxygen is subcooled to 55 K. The total I_{sp} of the integrated propulsion system is given by

$$I_{\Sigma} = \frac{I_{TJ}(K_A \varphi + \xi) + I_{LRE}(1 - \xi)(K_X + 1)}{1 + K_A \varphi + K_X(1 - \xi)} \quad (2)$$

where $I_{TJ} = R_{TJ}/(G_H^{TJ} + G_{OX})$ is the DCTJ I_{sp} and I_{LRE} is the LRE I_{sp} .

A fraction of turbojet thrust in total thrust at sea-level conditions is

$$DOL = 1 - \frac{I_{LRE}(1 - \xi)(K_X + 1)}{I_{\Sigma}[1 + K_A \varphi + K_X(1 - \xi)]} \quad (3)$$

The second important parameter along with I_{sp} is the thrust-to-weight ratio of the propulsion system:

$$T/W = 1 / \left\{ \frac{\bar{M}_A^{TJ} K_{A0}}{I_{\Sigma} [1 + K_{A\psi} + K_X (1 - \xi)]} + \frac{1 - DOL}{(T/W)_{LRE} \psi} \right\} \quad (4)$$

where \bar{M}_A^{TJ} is the mass of the DCTJ per 1 kg/s of airflow and $(T/W)_{LRE}$ is the LRE's thrust-to-weight ratio. The total mass of the turbojet includes the masses of the air intake, precooler, turbo-machinery, afterburner, and nozzle.

Propulsion system efficiency was analyzed in terms of effective I_{sp} (I_{sp}^E), which appeared to be a very efficient comparison tool. Effective I_{sp} provides a relation between local values of I_{sp} , vehicle drag, and engine thrust:

$$I_{sp}^E = I_{\Sigma} (1 - X/R) \quad (5)$$

Main Assumptions

The main assumptions of the current study are as follows:

1) The vehicle is currently intended for vertical takeoff (VTO) with a vehicle take off thrust-to-weight ratio of 1.3.

2) The combined cycle includes a throttlable LRE of the RL10 type. Instead of throttling ability, a different number of engines of the LRE cluster could be used (e.g., use of two engines in clusters of three is equivalent of 67% throttling).

3) The overall equivalence mixture ratio in the DCTJ was kept constant and equal to unity during acceleration. Other combinations were shown to be losers in terms of launcher efficiency.

4) The design point of the precooler corresponds to SLS conditions. The initial air temperature behind the compressor was $T_a = 110$ K, and the initial pressure recovery factors for air intake and precooler were $\sigma_{in} = 0.95$ and $\sigma_{pc} = 0.85$. The air intake pressure recovery factor profile along the trajectory was taken close to the MIL-SPEC standard.

5) The compressor pressure ratio at SLS conditions was taken as $\pi_c = 30$. Low total compression work allows a single spool compressor at this ratio.

6) The compressor and turbine efficiencies were assumed as $\eta = 0.82$.

7) Carbon-fiber-reinforced plastic (CFRP) with the density $\rho = 2000$ kg/m³ was assumed as the material that makes up 50% of the compressor rotor and stator pieces, as well as the precooler shell.

8) A shell-and-tube precooler of original configuration was selected. Stainless-steel tubes of 2 mm outer diameter with wall thickness 0.1 mm were considered.

9) Subcooled LOX at 55 K is injected in front of the precooler in the amount of 10% of the airflow from SLS static conditions up to Mach ≈ 0.8 and an altitude of $H \approx 3.5$ km to prevent precooler icing and increase initial DCTJ thrust.

10) An expandable dual-position bell nozzle was used for the LRE, and a self-adjusted flow using the vehicle afterbody was assumed for the DCTJ.

11) In all of the calculations, the vehicle structure index was equal to 19 kg/m².

Other assumptions can be found in following sections.

Effective I_{sp} Comparison

Equation (5) gives the definition of the so-called I_{sp}^E , which is the function of I_{sp} and vehicle drag-to-thrust ratio. This parameter (not I_{sp}) is in combination with the engine specific weight define launcher efficiency. Indirectly (through vehicle drag, which is particularly dependent on the vehicle mass/volume ratio or average vehicle density), I_{sp}^E also includes the overall oxygen/hydrogen ratio, which drops along with a K_{A0} increase.

Figure 3 shows I_{sp}^E vs flight Mach number for an all-rocket launcher and a family of curves for the KLIN launcher with the initial air-to-hydrogen ratio $K_{A0} = 6$. Curves in this family differ

Table 1 DCTJ parameters at SLS

Station in Fig. 4	Temperature, K	Pressure, bar
1	243	0.92
2	110	0.782
3	331	23.5
4	1451	22.3
5	1229	12.2
6	2505	11.8

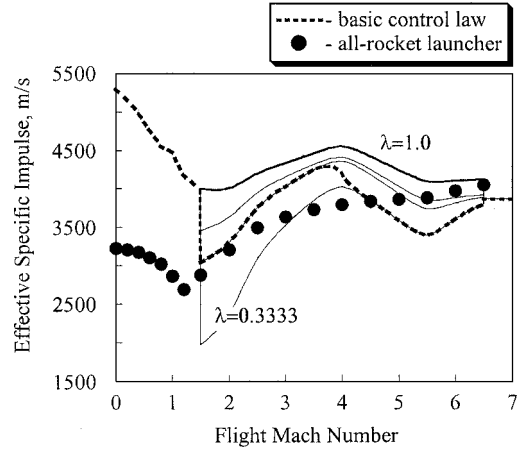


Fig. 3 Comparison of the I_{sp}^E .

by the rocket engine control law characterized by the rocket engine throttling factor λ . In Fig. 3 the throttling factor varies in the range of $\lambda = 0.3333 - 1.0$. The latter case means that the rocket engine operates with full thrust throughout the trajectory. The dotted line corresponds to case, which showed the best vehicle efficiency in previously conducted analyses. This case is characterized by full thrust LRE operation at the initial acceleration to Mach 1.5, 50% LRE throttling (I_{sp} increases by 15%), and further LRE throttling to 33% at Mach 4.0 (I_{sp} increases by 11%). The DCTJ units in all considerations produces maximum possible thrust.

Initially, the intention of the LRE throttling was to increase launcher efficiency through I_{sp} increase. However, according to Fig. 3, LRE throttling has negative impact on I_{sp}^E because of significant thrust reduction (by 75 and 35% at Mach 1.5 and 4.0 correspondingly). At Mach > 4.5 , I_{sp}^E of such a controlled KLIN Cycle becomes lower than the pure LRE. It was concluded from Fig. 3 that for the KLIN Cycle with $K_{A0} = 6$, which provided the best launcher efficiency, the best control law would be $\lambda = \text{const} = 1.0$ (i.e., the LRE should operate with the full thrust during the combined-cycle mode because it provides the highest level of the I_{sp}^E). Specific engine weight for all cases shown in Fig. 3 is the same (except for the rocket engine).

A concluding calculation was conducted for the KLIN Cycle with $K_{A0} = 6$ and $\lambda = \text{const} = 1.0$.

DCTJ Sizing and Operation

Figure 4 shows a new configuration of the DCTJ drawn in the current study. It is a dimensional scheme with major units sizing for SLS thrust of 6.95 tons. Table 1 gives DCTJ parameters in the main stations as shown in Fig. 4. The following is a brief description of the parameters and processes at each station.

Station 1 (in front of precooler): The 243 K temperature is the result of subcooled oxygen (at 55 K) injection into standard temperature air (at 288 K) in the amount of 10% (Note: the oxygen injection system is not shown in Fig. 4). This approach allows the process to be conducted in the precooler with frozen out moisture and prevents icing.

Station 2 (behind precooler, in front of compressor): Airflow passes through the precooler and is chilled to 110 K with a pressure

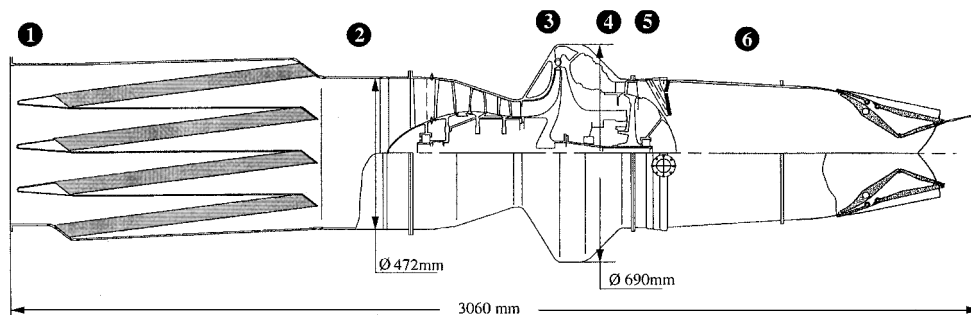


Fig. 4 Dimensional scheme of the 7-ton thrust DCTJ.

recovery factor of 0.85. Hydrogen discharge temperature from the pre-cooler is 85 K, and the pressure drop is slightly above 2%. The pre-cooler is the new four-“tooth” ZUB (ZUB is the Russian word for tooth that reflects the fact that this type of pre-cooler consists of several identical bundles of tubes.) configuration.

Station 3 (compressor discharge): The four-stage compressor (with one centrifugal stage) increases air pressure by a factor of 30 at the design point in SLS conditions. Air is heated in the compressor to 330 K at the design point. Along the trajectory pressure ratio significantly decreases. The maximum expected temperature behind the compressor is within 550 K and can be reduced if necessary. Therefore, lightweight composite materials or light alloys (aluminum based) can be utilized as the primary materials for compressor design.

Axial compressor stages are assumed to produce equal pressure ratio ($\pi_c = 1.92$ per stage). The average work per stage is as low as 28 kJ/kg, which is far below the typical maximum range of 50–70 kJ/kg per stage for turbojet compressors. The centrifugal stage produces a pressure ratio $\pi_c = 4.23$ and work 109 kJ/kg, which is also within modern level.

Station 4 (combustor exit): In the DCTJ combustor fuel lean combustion takes place to provide a combustion temperature $T < 1700$ K. Hydrogen flow through the combustor is variable depending on airflow and oxygen concentration in the airflow.

Station 5 (turbine exit): Only the one-stage turbine serves to drive the compressor. The expansion ratio in the turbine is nearly two, thus providing total work of the turbine stage of approximately 200 kJ/kg, which is far below maximum modern range of 400–500 kJ/kg.

Station 6 (afterburner): In the afterburner stoichiometric combustion of the triple mixture is completed after hydrogen addition. According to Table 1, temperature in afterburner can be as high as 2505 K. This shows that regenerative cooling of the afterburner is likely to be required.

Combustion products expand in the DCTJ convergent/divergent variable geometry nozzle. It could also be integrated with the vehicle afterbody (e.g., as an aerospike-type nozzle). Some geometry and mechanical parameters of the DCTJ at SLS conditions are listed here: relative hub diameter, 0.5; compressor tip speed, 350 m/s; compressor tip relative Mach number, 1.8; design spool speed, 14,686 rpm; and compressor inlet Mach number, 0.54. Moderate compressor tip speed corresponds to significant tip Mach number because of the very low speed of sound at temperatures of 110 K. This issue was studied in Ref. 4, which concluded that compressor efficiency and pressure ratio per stage will not be affected by a high tip Mach number.

Baseline KLIN Cycle

Engine performance and weight analyses are closely connected with trajectory analyses and launcher sizing. The KLIN Cycle (as described in this section) is a result of the trajectory analyses performed in the study.

It was proven in the efficiency analyses of a small RLV powered by the KLIN Cycle that minimums of the takeoff gross weight (TOGW), dry weight, and engine weight correspond to an initial air to hydrogen ratio $K_{40} = 6.0$. This means that the optimal (for the considered mission) KLIN Cycle is more rocket dominated than

has been considered. In addition, mentioned minimums correspond to the KLIN Cycle operation mode without LRE throttling during simultaneous operation with the DCTJ because this mode provides the highest value of the I_{sp}^E [Eq. (6)]. This fact has four favorable results for the KLIN Cycle: 1) the baseline KLIN Cycle is simpler to control (compare thrust profiles in Fig. 2a and 2b); 2) a better air/hydrogen ratio is maintained during DCTJ operation at higher speed, which allows more favorable air and hydrogen temperatures at pre-cooler exits; 3) a higher initial LRE thrust fraction eliminates the necessity of a spare engine to provide adequate thrust after transition to the all-rocket mode resulting in a propulsion system mass saving; and 4) a lower optimal DCTJ thrust fraction reduces risks of KLIN Cycle development.

The following is a description of the baseline KLIN Cycle operation modes and the major internal parameters of the DCTJ. Major KLIN Cycle parameters were conventionally divided on propulsion performance (shown in Fig. 5) and internal engine parameters (shown in Fig. 6).

Once it was shown in the launcher analyses that it is not necessary to throttle the LRE after initial acceleration, control law of the referenced KLIN Cycle is similar to what is shown in Fig. 2 for the rocket-dominated KLIN Cycle. A new flight scenario is shown in Fig. 5a in terms of I_{sp} and relative thrust variations in acceleration. There are three distinctive operational modes.

Mode 1 (from takeoff to Mach = 0.8) corresponds to simultaneous operation of all DCTJ units with oxygen augmentation and all of the LRE units. Maximum absolute thrust required for VTO and moderate I_{sp} are produced. Subcooled oxygen injection in the amount of 10% of the airflow in front of pre-cooler prevents icing and provides an approximately 20% DCTJ thrust increase with the same engine mass.

Mode 2 (in the range of Mach = 0.8–6.5) begins after oxygen injection is cutoff. Initially, thrust slightly decreases as I_{sp} increases (Fig. 5a). As the chosen trajectory provides significant airflow increase through the turbomachinery (Fig. 6a) up to Mach 4, I_{sp} increases and remains rather high up to this flight speed. Mach 4 was selected as the design point for air intake. This means that the maximum capture area of the variable geometry air inlet is designed for Mach 4, and further acceleration at higher altitude results in an airflow decrease through the air inlet. In other words, the air inlet is an airflow limiter after Mach 4 as turbomachinery is before Mach 4. To support turbomachinery operation at Mach > 4.0, actual spool speed should be gradually reduced (as shown in Fig. 6a).

Hydrogen flow is also reduced at a higher Mach number to provide stoichiometric combustion in the DCTJ. In the beginning of Mode 2, DCTJ thrust fraction DOL decreases along with hydrogen fraction for the DCTJ ξ (Fig. 5d) and then remains nearly constant up to Mach 4. Beyond Mach 4 the DCTJ thrust fraction in total KLIN Cycle thrust (DOL) sharply decreases to approximately 7% at Mach 6.5. A very smooth acceleration not exceeding 1.5 g is typical for the combined mode operation, and it is two times lower than in the all-rocket case.

Mode 3 (from Mach 6.5 to orbital speed), a pure rocket mode, begins after DCTJ cutoff, and LRE sole operation continues. The vehicle thrust-to-weight ratio should be equal to or greater than unity from the beginning of this operational mode. To meet this condition,

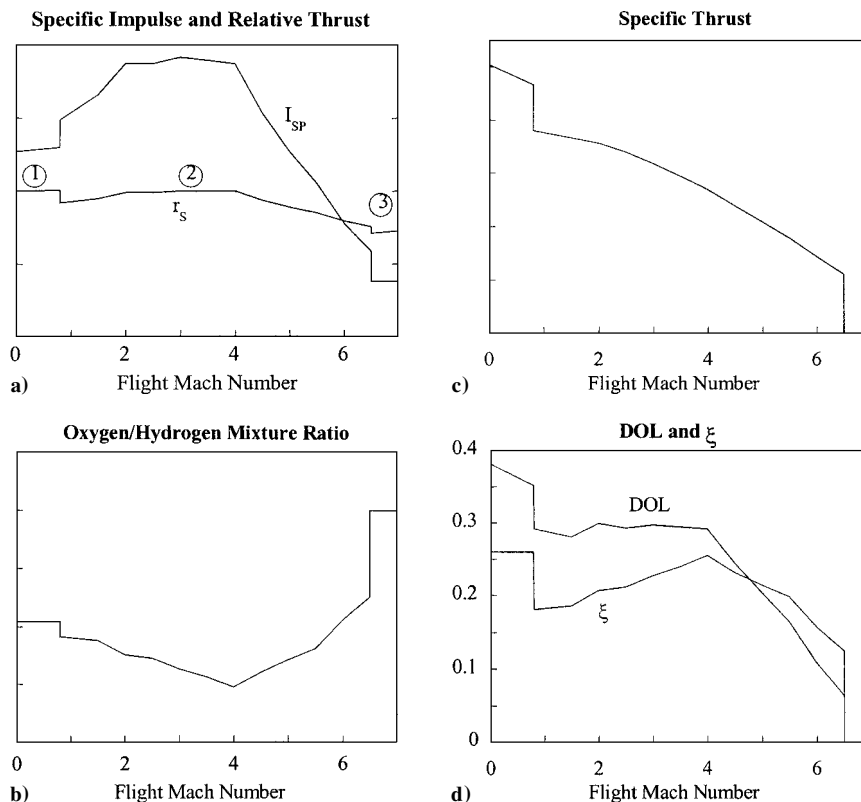


Fig. 5 Performance of the reference KLIN Cycle.

spare LRE unit(s) were included in the previous KLIN Cycle configurations, which were activated in this mode. This resulted in higher launcher weight and lower efficiency. In the current referenced case a spare LRE is not required because of rather high LRE fraction in the initial thrust. At Mach 6.5, after transition on all-rocket mode, vehicle thrust-to-weight ratio is approximately 1.3.

Additional comments to Figs. 5 and 6 are in order. The referenced KLIN Cycle provides rather moderate I_{sp} at an unusually high rocket-based combined cycle (RBCC) thrust profile (Fig. 5a). Thrust changes range from 76–101% of the SLS thrust. Figure 5b shows a profile of the oxygen/hydrogen mixture ratio. Oxygen and hydrogen flow rates include total LRE and DCTJ consumption. A mixture ratio obtained for the referenced cycle varies from 4.5 to 5.5 in the combined-cycle mode is much higher than in previous studies where it was in the range of 0–4 (0 corresponds to DCTJ sole operation). This factor is favorable for launcher efficiency because it reduces launcher volume and corresponding drag.

Figure 5c shows DCTJ specific thrust (i.e., thrust per 1 kg/s of air-flow). Sea-level static specific thrust is higher than 2000 m/s, which is a uniquely high level. Those modern turbfans with ultra low bypass ratios provide specific thrust of 1000–1200 m/s. The only fabricated and tested precooled turbomachine—the ATREX engine—reached 700 m/s, which the DCTJ provides at Mach 5.5. This unique level of specific thrust, along with very comfortable conditions in the compressor inlet (air temperature in front of compressor is shown in Fig. 6b), allows a very high thrust-to-weight propulsion system design. DCTJ contribution to SLS thrust $DOL = 38\%$ (Fig. 5d), as it consumes approximately 26% of the total hydrogen flow.

One of the important internal parameters is turbine inlet temperature. Its variation with flight Mach number is shown in Fig. 6c. It can be seen that the turbine temperature is within the declared upper limit of 1700 K at all times. It slightly exceeds this limit and reaches 1720 K at Mach 4. This excess can be easily offset by appropriate DCTJ control, or limited extension by 20 K can be discussed. DCTJ performance can be substantially improved if control law providing $T_T = \text{const}$ is applied. In this case an assumed limit of 1700 K can be kept from the SLS (currently SLS $T_T = 1450$ K). This will result in substantial DCTJ thrust and thrust-to-weight ratio increase.

According to Fig. 6b, the maximum hydrogen temperature reached after the precooler is 567 K at Mach 5.5–6.0. The possibility to use hydrogen at such temperatures as rocket combustor coolant can be confirmed in detailed LRE analyses. If necessary, several measures to reduce this temperature can be offered.

Figure 6d shows that ideally the DCTJ requires the nozzle area ratio to vary in the range of 2.5 to 20 and higher. The possibility of providing such area ratios and its impact on nozzle mass should be examined in further studies. A higher nozzle area ratio can be provided by nozzle integration into the vehicle afterbody. In this case flow self-adjustment will control the expansion process.

Figure 6e shows the profile of the relative pressure behind compressor of the DCTJ (SLS pressure is equal 23.5 bar and taken as 1.0 in Fig. 6e). Maximum pressure increase (44%) corresponds to Mach 4. If this pressure peak is not acceptable from the DCTJ perspective, it can be easily shaved (at the expense of DCTJ thrust) by several means such as an artificial pressure drop increase in the air inlet or spool speed reduction. Other critical parameters, for example DCTJ turbine inlet temperature (Fig. 6c), can also be traded for current engine efficiency.

To conclude the referenced KLIN Cycle analyses, it should be noted that the high efficiency of the KLIN launcher is a result of the synergy of the engine I_{sp} , high thrust profile (these two provide I_{sp}^E increase by more than 20% compared to an all-rocket launcher), oxygen/hydrogen mixture ratio higher than for the turbojet-dominated KLIN Cycle, and a very high engine thrust-to-weight ratio (for combined cycles) of 28–33.

It was shown in the described phase of the efficiency analyses of a small RLV powered by the KLIN Cycle that minimum values of gross takeoff weight, dry weight, and engine weight correspond to the initial air to hydrogen ratio $K_{A0} = 6.0$. This means that the optimal (for the considered mission) KLIN Cycle is more rocket dominated than has been already considered. In addition, stated minimums correspond to the KLIN Cycle operation mode without LRE throttling during simultaneous operation with the DCTJ because this mode provides the highest value of the I_{sp}^E . This fact has four favorable results for the KLIN Cycle: 1) the baseline KLIN Cycle is simpler to control; 2) a better air/hydrogen ratio is maintained

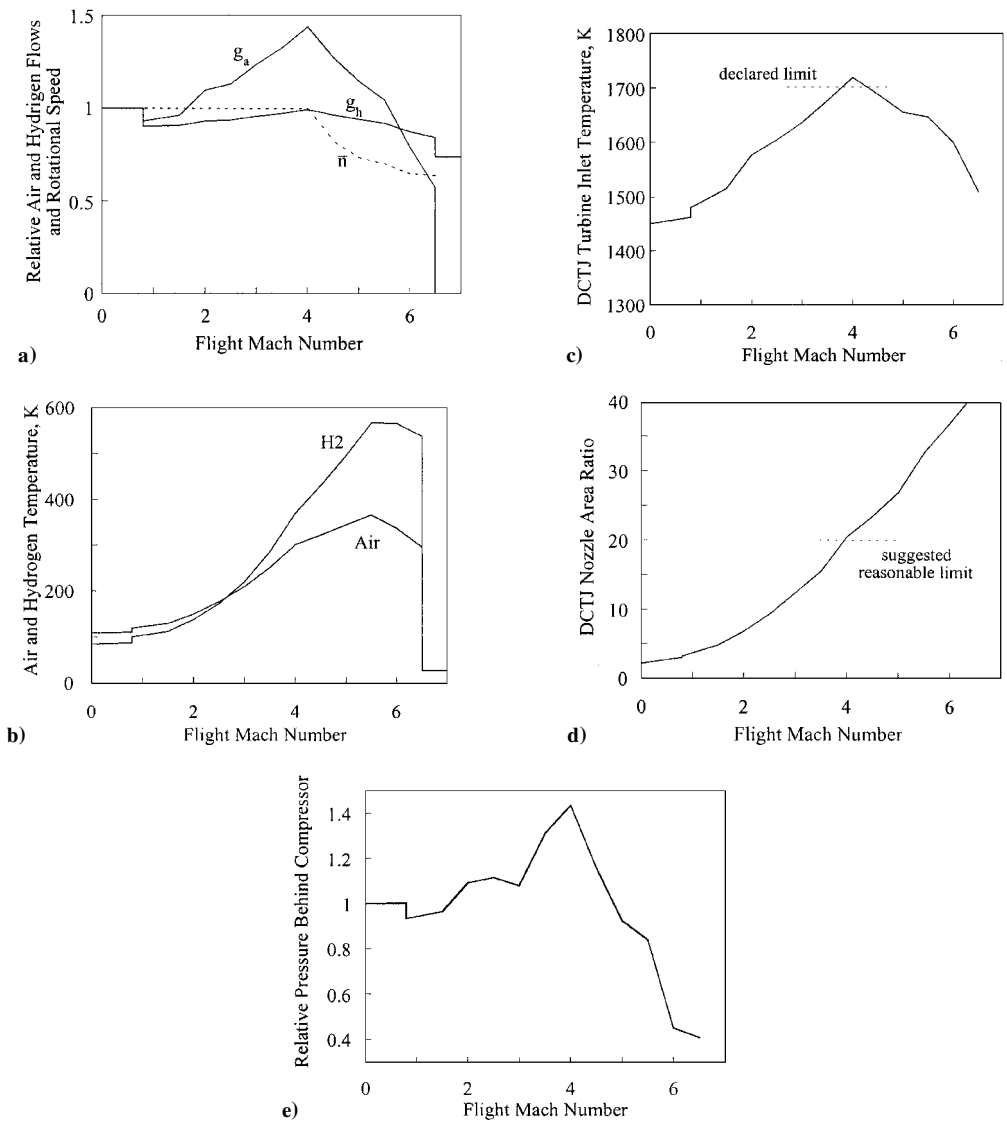


Fig. 6 Internal parameters of the reference KLIN Cycle: a) relative air, hydrogen flows, spool speed vs flight Mach number; b) air, hydrogen temperature at precooler exit; c) DCTJ turbine inlet temperature; d) DCTJ nozzle area ratio; and e) relative pressure behind compressor.

during DCTJ operation at higher speed, which allows for more favorable air and hydrogen temperatures at the precooler exits; 3) a higher initial LRE thrust fraction eliminates the necessity of a spare engine to provide adequate thrust after transition to the all-rocket mode, thereby resulting in a propulsion system mass saving; and 4) a lower optimal DCTJ thrust fraction reduces risks of KLIN Cycle development.

Summary of KLIN Launcher Analyses

The trajectory was determined using an optimum trajectory program that incorporated an engine cycle description and a sizing routine based on the one documented in *Hypersonic Convergence*.⁵ For the part of the flight that uses aerodynamic lift, the program uses the technique maximizing the specific excess power, namely,

$$P_s = V[(T - D)/W] \tag{6}$$

This is analogous for a minimum fuel climb for a high-performance combat aircraft.

The trajectory-averaged characteristics, weight ratio, oxidizer-to-fuel ratio, propellant density, and thrust-to-drag ratio were used as inputs into sizing program from Ref. 1 to confirm the vehicle size and weight. The sizing program from Ref. 5 simultaneously solves

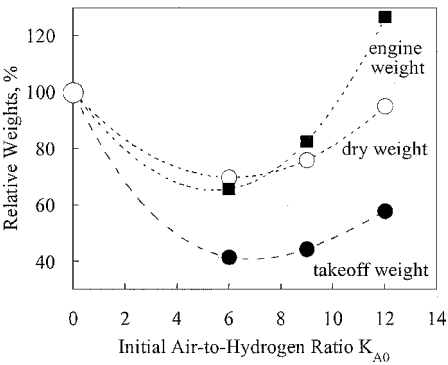


Fig. 7 Comparison of the weights of all-rocket launcher and the KLIN Cycle launcher as a functions of the air-to-hydrogen ratio.

the governing weight and volume equations. This procedure was done initially for original KLIN cases provided for a blended-body configuration concept. The analysis identified the KLIN Cycle that resulted in the smallest, lightest launcher.

A summary of results is shown in Fig. 7. The relative TOGW, dry weight, and propulsion system weight are plotted vs air-to-hydrogen ratio. Corresponding weights of the all-rocket launcher are taken as 100%. As Fig. 7 shows, the minimum TOGW would

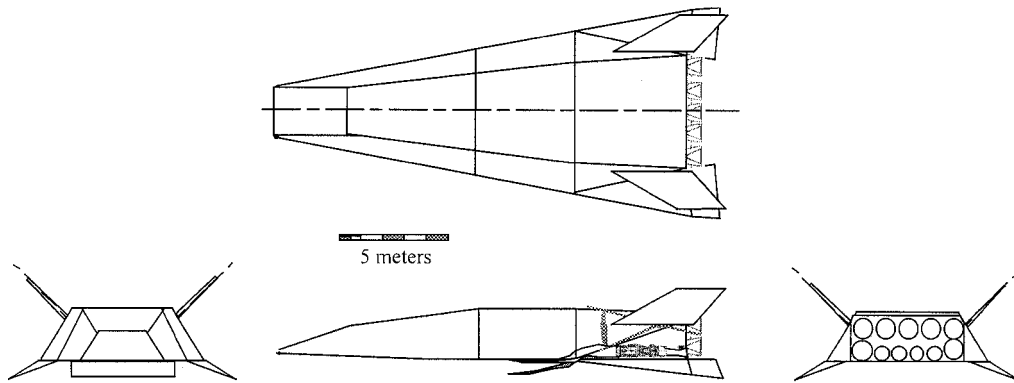


Fig. 8 KLIN Cycle-powered small satellite launcher.

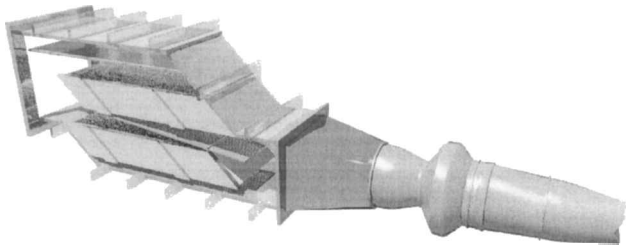


Fig. 9 DCTJ demonstrator.

be approximately 40%, and the dry weight and engine weight would be 70% of the corresponding weights of an all-rocket system. These minimums are rather gentle, and one may see that in the range of $K_{A0} = 5-8$, the KLIN Cycle launcher masses do not change too much. The minimum of the launcher dry weight corresponds to the DCTJ contribution in SLS thrust $DOL = 30-45\%$.

Strictly speaking, the KLIN Cycle launcher and all-rocket points in Fig. 7 cannot be connected by one curve because the KLIN Cycle launcher and the all-rocket launcher were evaluated for different trajectories. It is done only for visualization purposes. The impact of the values of K_{A0} in the range of 5–8 is minimal. The system designer has the freedom to choose the combinations of turbojets and rockets from available engines within this range. This provides a significant flexibility to integrate the launcher from available engines.

Following confirmation of the trajectory results for the KLIN Cycle, a parametric investigation was completed to identify the minimum weight and size of a practical vehicle suitable for a small satellite launcher powered by the KLIN Cycle propulsion system. This involved three steps: 1) evaluating different configuration concepts, 2) evaluating the impact of slenderness on the selected concept, and 3) examining the geometry to minimize weight and size. The resulting analysis identified a spatular trapezium as the best configuration for a practical small satellite launcher (Fig. 8). For the 150-kg small satellite payload, the resulting launcher was 20 m in length with a dry weight of 12 tons, a gross weight of 62 tons with planform area of 100 m², and a total volume of 160 m³ (approximate numbers are given). This configuration required seven RL10-type rocket engines with 7.7 tons SLS thrust each and four turbojets of 6.5 tons SLS thrust each.

Major observations from the trajectory and sizing study are as follows:

- 1) The configuration concept can result in a factor of two for size and weight.
- 2) Too slender a vehicle greatly increases weight.
- 3) The baseline configuration is a FDL-7 type trapezoidal hypersonic glider.

4) A spatular nose configuration permits greater volume at the same drag.

5) A spatular nose configuration reduces weight and size.

6) The KLIN Cycle sizing data are very consistent with prior demonstrator sizing results (Ref. 6).

7) The KLIN Cycle small satellite launcher is smaller and lighter than a corresponding RBCC powered demonstrator that operates at a higher airbreathing speed.

8) The availability of both turbojet engine and expander cycle rocket engines in the usable thrust class make the KLIN Cycle an attractive option for an SSTO demonstrator and small satellite launcher. Currently, pre-cooler design is being developed along with the test plan, which includes demonstration of the reliable pre-cooler operation is relevant conditions and ways to resolve main operational issues.

Figure 9 shows a pre-cooler assembly with one of the existing small turbine engines.

Conclusions

A KLIN Cycle baseline VTO SSTO RLV to deliver 330-lb payload to low Earth orbit was sized at TGOW 62 tons and a dry weight of 12 tons. The propulsion system configuration for the launcher has been defined. It includes seven RL10-type engines with 7.7 tons SLS thrust each and four DCTJs with 6.5 tons SLS thrust each.

The performance of the expander cycle rocket engine of the RL10 type can benefit from integration into the KLIN Cycle. Because of additional heating of the hydrogen fuel, it is possible to increase LRE I_{sp} by approximately 3% and thrust by approximately 16% (if turbopump control by +20% is assumed) with the same hardware. These advantages significantly offset the drawbacks of low chamber pressure LRE use in SLS conditions.

The DCTJ sizing was completed. Three new types of pre-coolers were examined. A four-“tooth” ZUB-type pre-cooler was selected for further DCTJ analyses and modeling.

The optimum KLIN Cycle corresponds to an initial air-to-hydrogenation of $K_{A0} = 6$. The thrust-to-weight ratio of this engine was estimated at 33.1 (if based on an LRE with $T/W = 43.6$). The most simple LRE control law (with full thrust) is the most efficient for the referenced KLIN Cycle, as it provides the highest profile of effective specific impulse for $K_{A0} = 6$.

The KLIN Cycle, based upon an RL10 rocket engine, makes a small reusable launcher of the BANTAM-class payload feasible and economically attractive and is within the capability of today's industry. This KLIN Cycle will create a new market of on-demand small payload launch services much like a space-launched Federal Express® or United Parcel Service®.

Acknowledgment

This study was conducted under U.S. Air Force Small Business Innovative Research Contract F04611-99-C-0047.

References

¹“Maintaining U.S. Leadership in Aeronautics. Breakthrough Technologies to Meet Future Air and Space Transportation Needs and Goals,” National Research Council, National Academy Press, Washington, DC, 1998.

²Balepin, V., Maita, M., and Murthy, S. N. B., “Third Way of Development of SSTO Propulsion,” *Journal of Propulsion and Power*, Vol. 17, No. 5, 1999, pp. 99–104.

³Tanatsugu, N., Balepin, V., Sato, T., Mizutani, T., Hamabe, K., and Tomike, J., “ATREX Engine Development: First Practical Experience of Precooled Turbomachinery,” *Proceedings of the 5th Association Aeronau-*

tique et Astronautique de France International Symposium Propulsion in Space Transportation, Paris, France, 1996, pp. 19.25–19.29.

⁴Balepin, V., and Breugelmans, F., “Combined Cycle for SSTO Rocket: Definition of the Key Technologies,” *Proceedings of the XIII International Society for Air Breathing Engines Symposium*, edited by F. S. Billig, AIAA, Chattanooga, TN, 1997, pp. 987–994.

⁵Czysz, P., *Hypersonic Convergence*, Vol. 1–10, 8th ed., Parks College of Engineering and Aviation, St. Louis Univ., MO, Dec. 1998.

⁶Czysz, P., Froning, A., David, H., and Longstaff, R., “A Concept for an International Project to Develop a Hypersonic Flight Test Vehicle,” AIAA Paper 97-2808, July 1997.